Supporting Information

Anticancer Organorhodium and -iridium Complexes with Low Toxicity in vivo but High Potency *in vitro*: DNA Damage, Reactive Oxygen Species Formation, and Haemolytic Activity

Shahida Parveen,[a] Muhammad Hanif,[a]* Euphemia Leung,[b] Kelvin K. H. Tong,[a] Annie Yang,[c] Jonathan Astin,[c] Gayan H. De Zoysa,[a] Tasha R. Steel,[a] David Goodman,[a] Sanam Movassaghi,[a] Tilo Söhnel,[a] Vijayalekshmi Sarojini,[a] Stephen M. F. Jamieson,[b] Christian G. Hartinger[a]*

[a.] School of Chemical Sciences, University of Auckland, Private Bag 92019, Auckland 1142, New Zealand.
[b.] Auckland Cancer Society Research Centre, University of Auckland, Private Bag 92019, Auckland 1142, New Zealand.
[c.] Department of Molecular Medicine and Pathology, University of Auckland, Private Bag 92019, Auckland 1142, New Zealand.

Table of Contents

Experimental

Materials and methods

All air-sensitive reactions were carried out under nitrogen in standard Schlenk flasks. 3-Hydroxy-2-methyl-4(1H)-pyrone (maltol), 1,4-butanediamine, 1,6-hexanediamine, 1,8-octanediamine and 1,12-dodecanediamine from Sigma, ruthenium(III) chloride hydrate (99%), Rhodium(III) chloride hydrate (99%) , Irridium(III) chloride hydrate (99%) from Precious Metals Online, and sodium methoxide from Fluka. Dichloromethane (DCM), diethyl ether (Et_2O), acetonitrile (ACN), chloroform and tetrahydrofuran (THF) were dried through a solvent purification system (LC Technology Solutions Inc., SP-1 solvent purifier) and transferred into Schlenk flasks that were dried under vacuum and degassed with N_2 prior to use. Ethanol (EtOH) and methanol (MeOH) were dried over activated molecular sieves (3 Å) in a N_2 Erlenmeyer flask for two days prior to use.

Bis[dichlorido(η^6-*p*-cymene)ruthenium(II)],[1] bis[dichlorido(η^5-pentamethylcyclopentadienyl)rhodium(III)],[2] bis[dichlorido(η^5-pentamethylcyclopentadienyl)iridium(III)],[3] 1,4-bis[3-benzyloxy-2-methyl-4(1*H*)-pyridinon-1-yl]butane **L^4**,[4-6] 1,6-bis[3-benzyloxy-2-methyl-4(1*H*)-pyridinon-1-yl]hexane **L^6**,[4-6] 1,8-bis[3-benzyloxy-2-methyl-4(1*H*)-pyridinon-1-yl]octane **L^8**,[4-6] 1,12-bis[3-benzyloxy-2-methyl-4(1*H*)-pyridinon-1-yl]dodecane **L^{12}**,[4-6] and 1,12-bis{chlorido[5-(oxo-κ*O*)-2-methyl-4-(1*H*)-pyridinonato-κ*O4*](η^6-*p*-cymene)ruthenium(II)}dodecane **Ru^{12}** [4-6] were prepared following literature procedures.

Thin layer chromatography (TLC) was performed on aluminium sheets pre-coated with Merck silica gel 60 F254. ^{1}H NMR and ^{13}C{^{1}H} NMR spectra were recorded on a Bruker Avance spectrometer at AVIII 400 MHz at ambient temperature at 400.13 MHz (^{1}H) and 100.61 (^{13}C{^{1}H}). For NMR experiments, D_2O, DMSO-d_6, and MeOH-d_4 were used as solvents. High-resolution mass spectra were recorded on a Bruker micrOTOF-Q II mass spectrometer in positive and negative ion electrospray ionization (ESI) mode. Elemental analyses were carried out on an Exeter Analytical Inc-CE-440 Elemental Analyzer.

General procedure for the synthesis of bimetallic Rh^{III} and Ir^{III} complexes

A solution of bis[dichlorido(Cp*)rhodium(III)] or bis[dichlorido(Cp*)iridium(III)] (1eq.) was added to a suspension of 1,n-bis[3-hydroxy-2-methyl-4(1*H*)-pyridinon-1-yl]alkane (**L^4**, **L^6**, **L^8** and **L^{12}**) (1 eq.) and sodium methoxide (2.2 eq.) in methanol and stirred under nitrogen atmosphere for 1–2 days. After completion of reaction, the reaction mixture was filtered to remove unconverted components and the solvent was removed under reduced pressure. Purification was performed by precipitation from dichloromethane with diethylether (1 : 1). Recrystallization was done by slow evaporation of methanol which afforded orange or red crystals.

1,4-Bis{chlorido[3-(oxo-κO)-2-methyl-4(1H)-pyridinonato-κO4](η^5-pentamethylcyclopentadienyl)rhodium(III)}butane, **Rh^4**

Complex **Rh^4** was synthesized by following the general procedure using 1,4-bis[3-hydroxy-2-methyl-4(1*H*)-pyridinon-1-yl]butane **L^4** (100 mg, 0.33 mmol), sodium methoxide (39 mg, 0.72 mmol) and $[Rh(Cp^*)Cl_2]_2$ (204 mg, 0.33 mmol).

Yield: 70% (196 mg, red crystals). Anal. found: C, 48.15; H, 5.90; N, 3.22; calcd for $C_{36}H_{48}N_2O_4Rh_2Cl_2 \cdot 0.5H_2O$: C, 48.34; H, 5.97; N, 3.13. MS (ESI$^+$) *m*/*z* 871.1027 (871.0993) $[M + Na]^+$, 813.1434 (813.1407) $[M - Cl]^+$, 389.0902 (389.0857) $[M - 2Cl]^{2+}$. ^{1}H NMR (400.13 MHz, MeOH-d_4, 25 °C) δ = 1.68 (brs, 30H, Cp^*), 1.74 (brs, 4H, H-2'), 2.44 (s, 6H, CH_3), 4.06 (brs, 4H, H-1'), 6.42 (d, ^3J = 7 Hz, 2H, H-5), 7.35 (d, ^3J = 7 Hz, 2H, H-5) ppm. $^{13}C\{^1H\}$ NMR (100.61 MHz, MeOH-d_4, 25 °C) δ = 8.8 (CH_3-Cp*), 12.0 (CH_3), 28.5 (C-2'), 55.2 (C-1'), 92.8 (C-Cp*), 110.8 (C-5), 134.0 (C-6), 134.8 (C-2), 160.9 (C-3), 175.3 (C-4) ppm.

1,6-Bis{chlorido[3-(oxo-κO)-2-methyl-4(1H)-pyridinonato-κO4](η^5-pentamethylcyclopentadienyl)rhodium(III)}hexane, **Rh^6**

Complex **Rh^6** was synthesized by following the general procedure using 1,6-bis[3-hydroxy-2-methyl-4(1*H*)-pyridinon-1-yl]hexane **L^6** (100 mg, 0.30 mmol), sodium methoxide (36 mg, 0.66 mmol) and $[Rh(Cp^*)Cl_2]_2$ (186 mg, 0.30 mmol).

Yield: 70% (184 mg, red solid). Anal. found: C, 51.94; H, 5.83; N, 3.18; calcd for $C_{38}H_{52}N_2O_4Rh_2Cl_2$: C, 52.01; H, 5.97; N, 3.19. MS (ESI$^+$) *m*/*z* 899.1338 (899.1306)

[M + Na]$^+$, 841.1751 (841.1720) [M – Cl]$^+$, 403.1036 (403.1013) [M – 2Cl]$^{2+}$. ^{1}H NMR (400.13 MHz, MeOH-d_4, 25 °C) δ =1.34 (brs, 4H, H-3'), 1.68 (brs, 34H, Cp*, H-2'), 2.43 (s, 6H, CH_3), 4.02 (t, ^3J = 7 Hz, 4H, H-1'), 6.38 (d, ^3J = 7 Hz, 2H, H-5), 7.32 (d, ^3J = 7 Hz, 2H, H-6) ppm. ^{13}C{^{1}H} NMR (100.61 MHz, MeOH-d_4, 25 °C) δ = 8.8 (CH_3-Cp*), 12.0 (CH_3), 26.9 (C-3'), 31.5 (C-2'), 55.7 (C-1'), 92.8 (C-Cp*), 110.7 (C-5), 134.0 (C-6), 134.7 (C-2), 160.8 (C-3), 175.1(C-4) ppm.

1,8-Bis{chlorido[3-(oxo-κO)-2-methyl-4(1H)-pyridinonato-κO4](η^5-pentamethylcyclopentadienyl)rhodium(III)}octane, **Rh^8**

Complex **Rh^8** was synthesized by following the general procedure using 1,8-bis[3-hydroxy-2-methyl-4(1*H*)-pyridinon-1-yl]octane **L^8** (100 mg, 0.28 mmol), sodium methoxide (33 mg, 0.61 mmol) and $[Rh(Cp^*)Cl_2]_2$ (173 mg, 0.28 mmol).

Yield: 70% (178 mg, red solid). Anal. found: C, 52.02; H, 6.43; N, 3.03; calcd for $C_{40}H_{56}N_2O_4Rh_2Cl_2 \cdot 0.75H_2O$. C, 52.27; H, 6.31; N, 3.05. MS (ESI$^+$) *m*/*z* 927.1648 (927.1619) [M + Na]$^+$, 869.2060 (869.2033) [M – Cl]$^+$, 417.1213 (417.1170) [M – 2Cl]$^{2+}$. ^{1}H NMR (400.13 MHz, MeOH-d_4, 25 °C) δ = 1.32 (brs, 8H, H-4', H-3'), 1.68 (brs, 34H, Cp*, H-2'), 2.44 (s, 6H, CH_3), 4.02 (t, ^3J = 7 Hz, 4H, H-1'), 6.39 (d, ^3J = 7 Hz, 2H, H-5), 7.33 (d, ^3J = 7 Hz, 2H, H-5) ppm. ^{13}C{^{1}H} NMR (100.61 MHz, MeOH-d_4, 25 °C) δ = 8.7 (CH_3-Cp*), 11.9 (CH_3), 27.1 (C-4'), 30.0 (C-3'), 31.7 (C-2'), 55.9 (C-1'), 92.8 (C-Cp*), 110.7 (C-5), 134.0 (C-6), 134.9 (C-2), 160.8 (C-3), 175.1 (C-4) ppm.

1,12-Bis{chlorido[3-(oxo-κO)-2-methyl-4(1H)-pyridinonato-κO4](η^5-pentamethylcyclopentadienyl)rhodium(III)}dodecane, **Rh^{12}**

Complex **Rh^{12}** was synthesized by following the general procedure using 1,12-bis[3-hydroxy-2-methyl-4(1*H*)-pyridinon-1-yl]dodecane **L^{12}** (100 mg, 0.24 mmol), sodium methoxide (28 mg, 0.53 mmol) and $[Rh(Cp^*)Cl_2]_2$ (148 mg, 0.24 mmol).

Yield: 60% (138 mg, red solid). Anal. found: C, 54.97; H, 6.72; N, 3.17; calcd for $C_{44}H_{64}N_2O_4Rh_2Cl_2$. C, 54.95; H, 6.71; N, 2.91. MS (ESI$^+$) *m*/*z* 983.2226 (983.2245) [M + Na]$^+$, 925.2651 (925.2659) [M – Cl]$^+$, 445.1478 (445.1483) [M – 2Cl]$^{2+}$. ^{1}H NMR (400.13 MHz, MeOH-d_4, 25 °C) δ =1.30 (d, ^3J = 7 Hz, 16 H, H-6', H-5', H-4', H-3'), 1.68 (brs, 34H, Cp*, H-2'), 2.45 (s, 6H, CH_3), 4.03 (t, ^3J = 7 Hz, 4H, H-1'), 6.41 (d, ^3J = 7 Hz,

2H, H-5), 7.35 (d, ^3J = 7 Hz, 2H, H-5) ppm. $^{13}C\{^1H\}$ NMR (100.61 MHz, MeOH-d_4, 25 °C) δ = 8.7 (CH_3-Cp*), 11.9 (CH_3), 27.3 (C-6'), 30.2 (C-5'), 30.5 (C-4', C-3'), 31.8 (C-2'), 55.9 (C-1'), 92.8 (C-Cp*), 110.7 (C-5), 134.0 (C-6), 134.9 (C-2), 160.8 (C-3), 175.1(C-4) ppm.

1,4-Bis{chlorido[3-(oxo-κO)-2-methyl-4(1H)-pyridinonato-κO4](η^5-pentamethylcyclopentadienyl)iridium(III)}butane, **Ir^4**

Complex **Ir^4** was synthesized by following the general procedure using 1,4-bis[3-hydroxy-2-methyl-4(1*H*)-pyridinon-1-yl]butane **L^4** (100 mg, 0.33 mmol), sodium methoxide (39.07 mg, 0.72 mmol) and $[Ir(Cp^*)Cl_2]_2$ (263 mg, 0.33 mmol).

Yield: 70% (237 mg, orange crystals). Anal. found: C, 41.10; H, 5.01; N, 2.82; calcd for $C_{36}H_{48}N_2O_4Ir_2Cl_2 \cdot H_2O$. C, 41.33; H, 4.82; N, 2.68. MS (ESI$^+$) *m*/*z* 1051.2202 (1051.2121) $[M + Na]^+$, 993.2572 (993.2545) $[M - Cl]^+$. ^1H NMR (400.13 MHz, MeOH-d_4, 25 °C) δ = 1.67 (s, 30H, Cp*), 1.78 (brs, 4H, H-2'), 2.46 (s, 6H, CH_3), 4.10 (brs, 4H, H-1'), 6.45 (d, ^3J = 7 Hz, 2H, H-5), 7.39 (d, ^3J = 7 Hz, 2H, H-5) ppm. $^{13}C\{^1H\}$ NMR (100.61 MHz, MeOH-d_4, 25 °C) δ = 9.1 (CH_3-Cp*), 11.9 (CH_3), 28.4 (C-2'), 55.2 (C-1'), 83.7 (C-Cp*), 110.7 (C-5), 134.5 (C-6), 135.5 (C-2), 162.6 (C-3), 176.3 (C-4) ppm.

1,6-Bis{chlorido[3-(oxo-κO)-2-methyl-4(1H)-pyridinonato-κO4](η^5-pentamethylcyclopentadienyl)iridium(III)}hexane, **Ir^6**

Complex **Ir^6** was synthesized by following the general procedure using 1,6-bis[3-hydroxy-2-methyl-4(1*H*)-pyridinon-1-yl]hexane **L^6** (100 mg, 0.30 mmol), sodium methoxide (36 mg, 0.66 mmol) and $[Ir(Cp^*)Cl_2]_2$ (239 mg, 0.30 mmol).

Yield: 70% (216 mg, orange solid). Anal. found: C, 43.07; H, 5.22; N, 2.44; calcd for $C_{38}H_{52}N_2O_4Ir_2Cl_2$: C, 43.21; H, 4.96; N, 2.65. MS (ESI$^+$) *m*/*z* 1079.2497 (1079.2434) $[M + Na]^+$, 1021.2897 (1021.2858) $[M - Cl]^+$, 492.1605 (492.1576) $[M - 2Cl]^{2+}$. ^1H NMR (400.13 MHz, MeOH-d_4, 25 °C) δ =1.28 (brs, 4H, H-3'), 1.68 (brs, 34H, Cp*, H-2'), 2.40 (t, ^3J = 7 Hz, 6H, CH_3-Cp*), 3.83 (brs, 4H, H-1'), 6.37 (d, ^3J = 7 Hz, 2H, H-5), 6.95 (d, ^3J = 7 Hz, 2H, H-6) ppm. $^{13}C\{^1H\}$ NMR (100.61 MHz, MeOH-d_4, 25 °C) δ = 9.1 (CH_3-Cp*), 12.0 (CH_3), 26.8 (C-3'), 31.5 (C-2'), 55.7 (C-1'), 83.7 (C-Cp*), 110.6 (C-5), 134.6 (C-6), 135.6 (C-2), 162.5 (C-3), 176.1 (C-4) ppm.

1,8-Bis{chlorido[3-(oxo-κO)-2-methyl-4(1H)-pyridinonato-κO4](η^5-pentamethylcyclopentadienyl)iridium(III)}octane, **Ir^8**

Complex **Ir^8** was synthesized by following the general procedure using 1,8-bis[3-hydroxy-2-methyl-4(1*H*)-pyridinon-1-yl]octane **L^8** (100 mg, 0.28 mmol), sodium methoxide (33 mg, 0.61 mmol) and $[Ir(Cp^*)Cl_2]_2$ (223 mg, 0.28 mmol).

Yield: 68% (178 mg, orange solid). Anal. found: C, 44.20; H, 4.92; N, 2.43; calcd for $C_{40}H_{56}N_2O_4Ir_2Cl_2$. C, 44.30; H, 5.21; N, 2.58. MS (ESI$^+$) *m*/*z* 1107.2809 (1107.2748) $[M + Na]^+$, 1049.3213 (1049.3172) $[M – Cl]^+$, 506.1768 (506.1733) $[M – 2Cl]^{2+}$. ^{1}H NMR (400.13 MHz, MeOH-d_4, 25 °C) δ = 1.26 (brs, 8H, H-4', H-3'), 1.70 (brs, 30H, Cp*), 1.77 (brs, 4H, H-2'), 2.44 (s, 6H, CH_3), 3.84 (t, ^3J = 7 Hz, 4H, H-1'), 6.42 (d, ^3J = 7 Hz, 2H, H-5), 6.95 (d,^3J = 7 Hz, 2H, H-5) ppm. ^{13}C{^{1}H} NMR (100.61 MHz, MeOH-d_4, 25 °C) δ = 9.1 (CH_3-Cp*), 12.0 (CH_3), 27.1 (C-4'), 29.9 (C-3'), 31.6 (C-2'), 55.9 (C-1'), 83.8 (C-Cp*), 110.5 (C-5), 134.6 (C-6), 135.7 (C-2), 162.5 (C-3), 176.1 (C-4) ppm.

1,12-Bis{chlorido[3-(oxo-κO)-2-methyl-4(1H)-pyridinonato-κO4](η^5-pentamethylcyclopentadienyl)iridium(III)}dodecane, **Ir^{12}**

Complex **Ir^{12}** was synthesized by following the general procedure using 1,12-bis[3-hydroxy-2-methyl-4(1*H*)-pyridinon-1-yl]dodecane **L^{12}** (100 mg, 0.24 mmol), sodium methoxide (28 mg, 0.53 mmol) and $[Ir(Cp^*)Cl_2]_2$ (191 mg, 0.24 mmol).

Yield: 60% (164 mg, orange solid). Anal. found: C, 45.97; H, 5.43; N, 2.79; calcd for $C_{44}H_{64}N_2O_4Ir_2Cl_2$. C, 46.34; H, 5.66; N, 2.46. MS (ESI$^+$) *m*/*z* 1105.3826 (1105.3799) $[M – Cl]^+$. ^{1}H NMR (400.13 MHz, MeOH-d_4, 25 °C) δ = 0.84 (m, 8H, H-6', H-5'), 1.26 (m, 16H, H-1', H-2', H-3', H-4'), 1.63 (brs, 34H, Cp*, H-2'), 2.40 (s, 6H, CH_3), 4.01 (t, ^3J = 7 Hz, 4H, H-1'), 6.36 (d, ^3J = 7 Hz, 2H, H-5), 7.30 (d, ^3J = 7 Hz, 2H, H-5) ppm. ^{13}C {1H} NMR (100.61 MHz, MeOH-d_4, 25 °C) δ = 9.2 (CH_3-Cp*), 11.9 (CH_3), 27.3 (C-6'), 30.2 (C-5'), 30.5 (C-4', C-3'), 31.8 (C-2'), 56.0 (C-1'), 83.8 (C-Cp*), 110.6 (C-5), 134.6 (C-6), 135.7 (C-2), 162.5 (C-3), 176.1 (C-4) ppm.

X-ray diffraction analysis

The X-ray diffraction data of **Rh⁴** and **Ir⁴** was collected on a Bruker Smart APEX II diffractometer with graphite-monochromatised Mo*Kα* radiation, λ_{Mo} = 0.71073 Å at 100 K. Data reduction was carried out using the SAINT program.[7] Semi-empirical absorption corrections were applied based on equivalent reflections using SADABS.[8] The structure solution and refinements were performed with the SHELXS-97, SHELXL-2016 and Olex2 program packages.[9,10]

Table S1. Crystal data and details of data collection for complex **Rh⁴** and **Ir⁴**.

	Rh⁴·4 H_2O	**Ir⁴**·2 CH_3OH
CCDC	1915580	1915581
Empirical formula	$C_{36}H_{48}Cl_2Rh_2N_2O_4$·4 H_2O	$C_{36}H_{48}Cl_2Ir_2N_2O_4$· 2 CH_3OH
M / g mol^{-1}	921.54	1092.14
T / K	100	100
Wavelength (Å)	0.71073	0.71073
Crystal size	0.36 × 0.22 × 0.12 mm	0.32 × 0.28 × 0.24 mm
Crystal system	triclinic	monoclinic
Space group	*P*-1	$P2_1/n$
a / Å	8.3327(3)	7.8857(2)
b / Å	8.6240(4)	14.3838(3)
c / Å	14.4874(6)	17.7206(5)
α / °	75.400(2)	90
β / °	76.174(2)	97.4552(14)
γ / °	76.504(2)	90
V / $Å^3$	961.52(7)	1992.99(8)
Z	1	2
D_c / mg m^{-3}	1.591	1.820
Absorption coefficient / mm^{-1}	1.049	6.850
F(000)	474	1068
Theta range for data collection/°	2.56 to 28.28	2.71 to 29.57
h range	-11 ≤ h ≤ 11	-10 ≤ h ≤ 10
k range	-11 ≤ k ≤ 11	-18 ≤ k ≤ 19
l range	-19 ≤ l ≤ 19	-24 ≤ l ≤ 24
Reflections collected / unique	22123 / 4737 [R(int) = 0.0416]	25662 / 5579 [R(int) = 0.0528]
Data / restraints / parameters	4737 / 0 / 241	5579 / 1 / 243
Goodness-of-fit on F^2	1.058	1.057
Final R indices [I>2sigma(I)]	R1 = 0.0335 wR2 = 0.0787	R1 = 0.0311 wR2 = 0.0643
R indices (all data)	R1 = 0.0391 wR2 = 0.0819	R1 = 0.0415 wR2 = 0.0680
Largest diff. peak and hole	2.01 and -0.79 e·A^{-3}	1.50 and -1.20 e·A^{-3}

Table S2. Selected bond lengths [Å] of **Rh[4]** and **Ir[4]** in comparison to structurally related **Ru[6]**.

Bond	Rh[4]	Ir[4]	Ru[6] [a]
M–Cl1	2.4402(7)	2.4235(10)	2.419(1)
M–O1	2.085(2)	2.093(2)	2.073(3)
M–O2	2.112(2)	2.120(2)	2.103(3)
C3–O1	1.344(3)	1.320(4)	1.349(5)
C4–O2	1.296(3)	1.307(4)	1.306(5)
C3–C4	1.416(4)	1.425(5)	1.409(6)

[a] taken from ref. [6]

Stability in aqueous solution

The aqueous stability of **Rh[4]** and **Ir[4]** was studied by dissolving 1–2 mg/mL in D_2O (**Rh[4]**) or D_2O /d_4-MeOD (**Ir[4]**). ^{1}H NMR spectra were recorded after 0.5, 2, 24, 48, 72, 96 and 120 h. To initiate a chlorido/aqua ligand exchange, the complexes were treated with $AgNO_3$ (2 eq.) and the ^{1}H NMR spectra were recorded immediately after AgCl was filtered off.

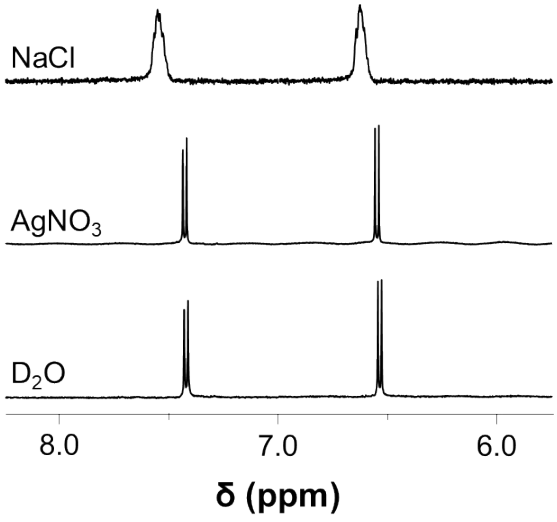

Figure S1. Stability study for **Rh[4]** in D_2O, after treatment with $AgNO_3$ and in D_2O with 100 mM NaCl by ^{1}H NMR spectroscopy.

Cyclic Voltammetry

Cyclic voltammetry experiments were performed at room temperature utilising a BAS CGME Controlled Growth Mercury Electrode cell stand at scan rates of 10, 20, 100 and 1000 mVs^{-1} with a glassy carbon working electrode, platinum auxiliary electrode and a silver wire as a quasireference electrode with the ferrocene/ferrocenium couple acting as an internal standard (calculated as: $[Fe(\eta^5\text{-}C_5H_5)_2]^{0/+}$ = +0.77 V vs NHE in DMF at 25 °C). All samples were degassed with nitrogen prior to measurement and maintained under a nitrogen atmosphere throughout at 5 mM concentration in DMF with 0.1 M tetrabutylammonium chloride as the supporting electrolyte.

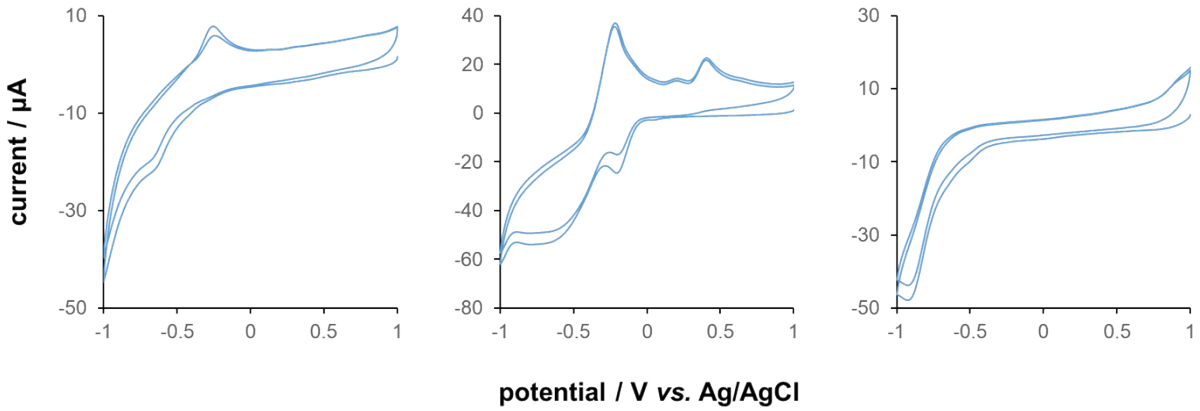

Figure S2. Cyclic voltammograms for **Ru**[12], **Rh**[12] and **Ir**[12], recorded at a scan rate of 100 mV/s at 5 mM concentration in DMF with tetrabutylammonium chloride.

Cell Cytotoxicity

HCT116, SW480 and NCI-H460 cells were supplied by ATCC, while SiHa cells were supplied from Dr. David Cowan, Ontario Cancer Institute, Canada. The cells were grown in αMEM (Life Technologies) supplemented with 5% foetal calf serum (Moregate Biotech) at 37 °C in a humidified incubator with 5% CO_2. The cytotoxicity was determined by the sulforhodamine B assay as described previously.[11]

Table S3. *In vitro* cytotoxic activity (mean IC_{50} values ± standard deviations) and the aqueous solubility of **Rh^4**, **Rh^6**, **Rh^8**, **Rh^{12}**, **Ir^4**, **Ir^6**, **Ir^8** and **Ir^{12}** in the human cancer cell lines HCT116 (colon), NCI-H460 (non-small cell lung), SiHa (cervix), and SW480 (colon) given in µM as determined by the SRB assay (exposure time 72 h, n = 3).

Compound	**Solubility (µM)**	**IC_{50} values / µM**			
		HCT116	NCI-H460	SiHa	SW480
Rh^4 [a]	943	52 ± 6	15 ± 1	25 ± 12	46 ± 2
Rh^6 [a]	899	31 ± 9	23 ± 2	36 ± 7	40 ± 10
Rh^8	672	6 ± 0.4 *,**	7 ± 1	11 ± 1 *,**	9 ± 1
Rh^{12}	586	0.20 ± 0.02 *,**,***	0.05 ± 0.01 *,**,***	0.46 ± 0.03 *,**,***	0.26 ± 0.07 *,**,***
Ir^4	636	61 ± 3	24 ± 5	28 ± 3	44 ± 10
Ir^6	496	14 ± 4	12 ± 3	17 ± 1	14 ± 3
Ir^8	438	10 ± 0.3 *,**	7 ± 1	14 ± 1	9 ± 1 *
Ir^{12}	237	0.38 ± 0.04*,**,***	0.21 ± 0.05 *,**,***	0.75 ± 0.1 *,**,***	0.88 ± 0.09 *,**,***

[a] n = 5; statistical analysis using the student t-test: *, $p < 0.05$ compared to **Rh^4** or **Ir^4**; **, $p < 0.05$ compared to **Rh^6** or **Ir^6**; *, $p < 0.05$ compared to **Rh^8** or **Ir^8**.

Aqueous solubility in water

For determining the aqueous solubility, a weighed sample of each complex was dissolved in a minimum amount of DMSO, which was diluted with deionized water to reach a final concentration of DMSO equal to 1%. The solution was visually inspected for any undissolved complex or suspension.

Calculated logarithmic octanol/water partition coefficient (clog*P*)

ChemBioDrawUltra 17.1 was used to estimate the lipophilicity based on calculated logarithmic octanol-water partition coefficients (clog*P*) of **L^{4}**, **L^{6}**, **L^{8}** and **L^{12}**.

Table S4. Calculated logarithmic *n*-octanol/water partition coefficients (clog*P*) for **L^{4}**, **L^{6}**, **L^{8}** and **L^{12}** in their protonated forms calculated with ChemDraw 17.1.

Compound	clog*P*
L^{4}	-2.57
L^{6}	-1.73
L^{8}	-0.90
L^{12}	0.77

ROS Induction

Intracellular ROS were detected with the cell-permeable fluorescent probe 2',7'-dichlorofluorescein diacetate (DCFDA; ABCAM) according to the manufacturer's instruction and following established protocol.[12] HCT116 cells (1×10^5 per sample) were harvested, incubated with 20 μM DCFDA in medium for 30 min in the dark at 37 °C. Cells were exposed to 100 μM of **Ru^{12}**, **Rh^{12}** and **Ir^{12}** for 1 h, and analysed immediately in a BD Accuri™ Flow Cytometer.

Flow cytometry

HCT116 cells (7.2 × 10^5 cells per well) were plated in 6-well plates overnight and incubated with **Ru[12]**, **Rh[12]**, **Ir[12]**, cisplatin (30 μM each), doxorubicin (1 μM), and camptothecin (1 μM) for 6 h. As described previously,[13] cells were harvested, fixed with 80% ethanol for 10 min, washed and resuspended in 1 mL of blocking buffer (1% FCS/PBS), and incubated with antibody to γH2AX (phosphorylated Ser139, clone JBW301; Millipore, USA) in blocking buffer (1 : 500 dilution) at room temperature for 2 h. Cells were washed, incubated with goat anti-mouse Alexa Fluor 488 Fab fragment secondary antibody (Invitrogen, New Zealand; 1 : 400 in blocking buffer for 1 h, at room temperature; dark), washed and resuspended in 1 mL of blocking buffer containing RNase (1 μg/mL) and propidium iodide (PI; 10 μg/mL) for 10 min at room temperature. Cells were analysed in Becton Dickinson BD Accuri C6 flow cytometer.

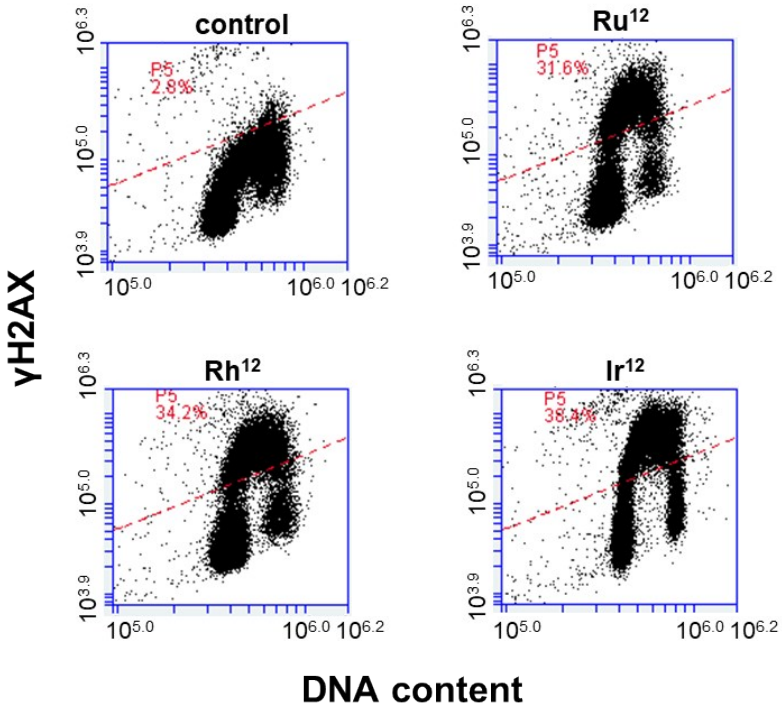

Figure S3. The expression of γH2AX in HCT116 cells exposed to **Ru[12]**, **Rh[12]**, and **Ir[12]** at 30 μM for 6 h. Statistical significance: $p < 0.05$, compared to control.

Haemolysis Assay

The haemolytic activity of the **Rh[12]**, **Ir[12]** and cisplatin was tested by determining the extent of hemoglobin release from erythrocyte suspensions of freshly collected mouse blood cells (2% vol/vol). The blood cells were centrifuged at 1000 × g for 5 min and the plasma was removed. The blood cells were washed with Tris buffer (10 mM Tris, 150 mM NaCl, pH 7.2) and afterwards suspended in 2% vol/vol of the Tris buffer. **Rh[12]**, **Ir[12]** and cisplatin at various concentrations ranging from 2 μM to 1 mM were dissolved in DMSO and Tris buffer (final DMSO less than 1%). The solutions (100 μL) were added to the suspended blood cells (100 μL) in 96-well plates and the plates were incubated for 1 h at 37 °C without agitation. Buffer solution and 1% Triton X-100 as negative and positive controls, respectively, were included in the assay. The samples were tested in triplicates. The plates were centrifuged at 3500 × g for 10 mins. The supernatant was transferred into separate 96 well plates and absorbance at 540 nm was measured with a microplate reader. The percentage haemolysis at each concentration was calculated from the following equation:

$$\% \text{ Haemolysis} = (A_{exp} - A_{Tris})/(A_{100\%} - A_{Tris}) \times 100 \quad (1)$$

Where A_{exp} is the experimental absorbance at 540 nm, A_{Tris} is the absorbance of the negative control and $A_{100\%}$ is the absorbance of the positive control that causes 100% lysis of RBCs present.

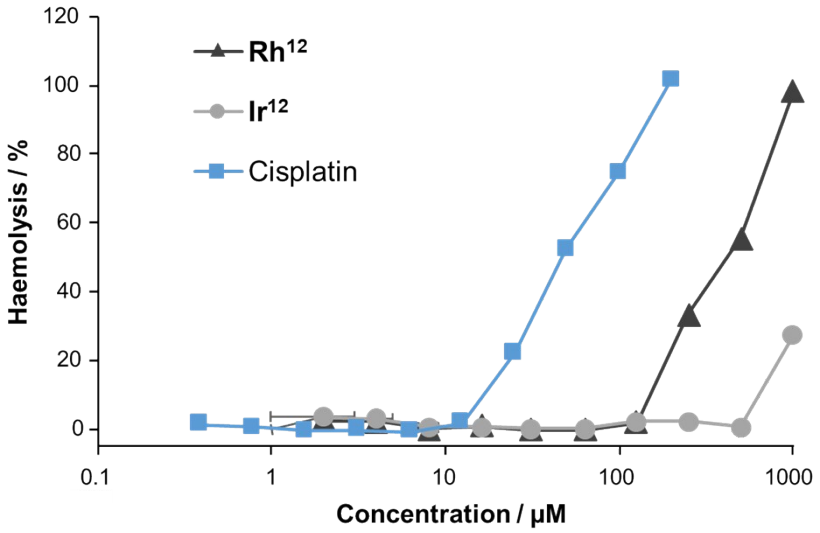

Figure S4. Percentage of haemolysis of mouse blood cells induced by **Rh^{12}** and **Ir^{12}** at various concentrations in comparison to cisplatin. The standard deviations for all data points were < 1.5% and therefore the error bars are not displayed.

Zebrafish experiments

In vivo assessment of **Rh^{12}** and **Ir^{12}** on the vascular development was performed on Friend leukaemia integration 1a transgenic zebrafish (*fli1a:EGFP*), which express GFP (green fluorescent protein) in the vasculature.[14] At 4 hours post-fertilization (hpf), 15–20 zebrafish embryos per experimental group were placed in E3 media (5 mL) supplemented with either vehicle (DMSO) or 0.5 µM of inhibitor and maintained in the dark. At 24 hpf, 0.003% (w/v) 1-phenyl-2-thiourea was added to inhibit pigment formation. At 48 hpf, zebrafish embryos were manually dechorinated, anaesthetised with 0.01% (w/v) tricaine (3-aminobenzoic acid ethyl ester) and mounted for imaging on a Nikon D-Eclipse C1 confocal microscope as previously described.[15]

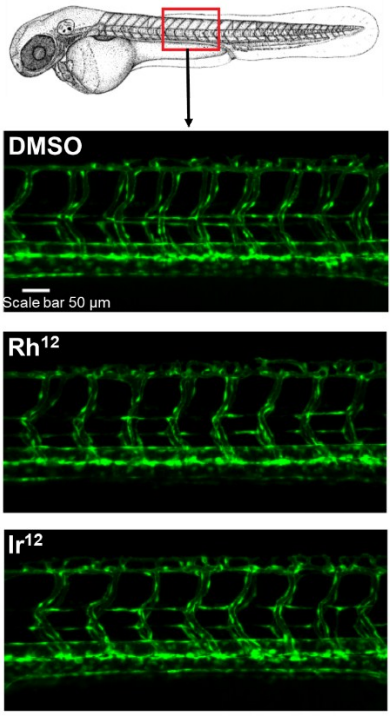

Figure S5. Confocal images of the developing trunk vasculature in 48 hpf (hours post-fertilization) in *fli1a:EGFP* zebrafish embryos (n > 20 for all treatment groups) treated with either vehicle (DMSO) or 0.5 µM of either **Rh^{12}** or **Ir^{12}**.

Statistical Analysis. All the IC_{50} data are given are mean ± standard deviation. The statistical analyses were performed using PRISM (GraphPad prism® software 8.0) with student's one-tailed paired t-test or the Mann-Whitney test. Statistical significance (p) values of < 0.05 were considered to be statistically significant.

NMR spectra of the synthesised compounds

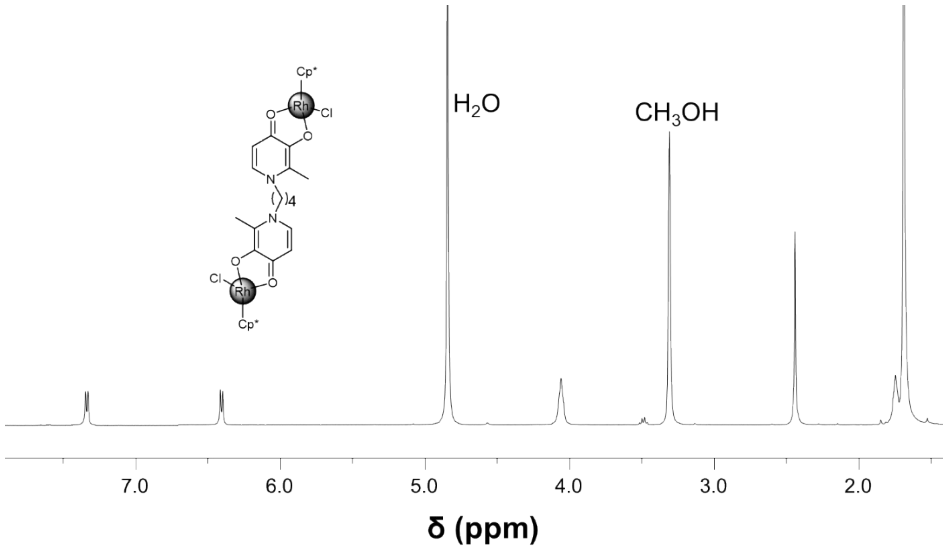

Figure S6. ^{1}H NMR spectrum for **Rh⁴** recorded in CD_3OD.

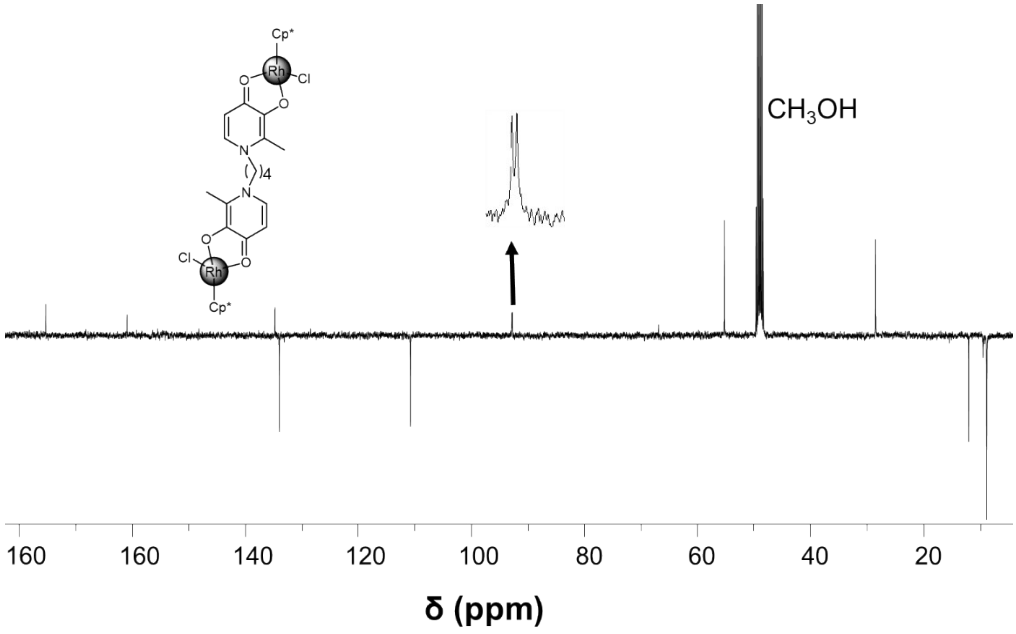

Figure S7. $^{13}C\{^{1}H\}$ NMR spectrum for **Rh⁴** recorded in CD_3OD.

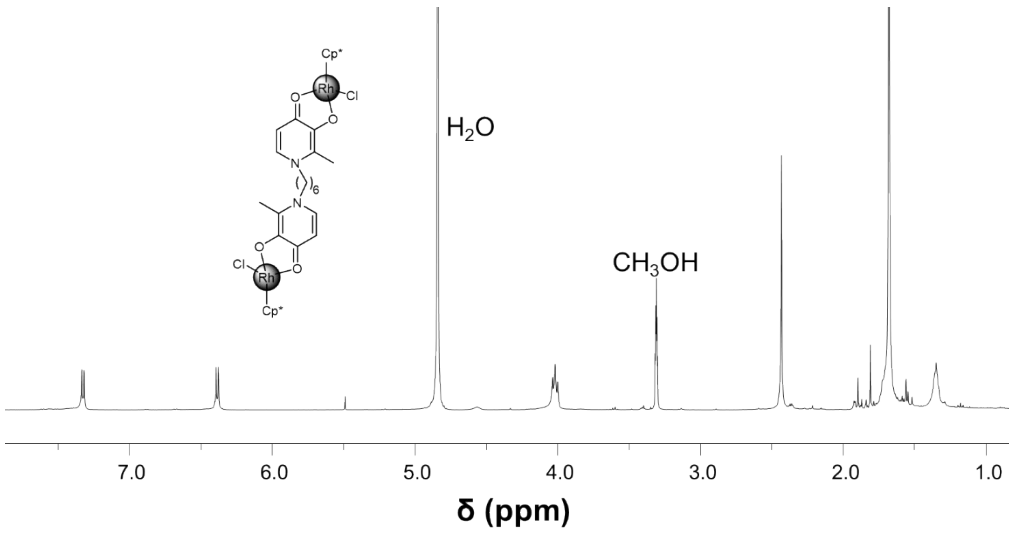

Figure S8. ^{1}H NMR spectrum for **Rh^{6}** recorded in CD_3OD.

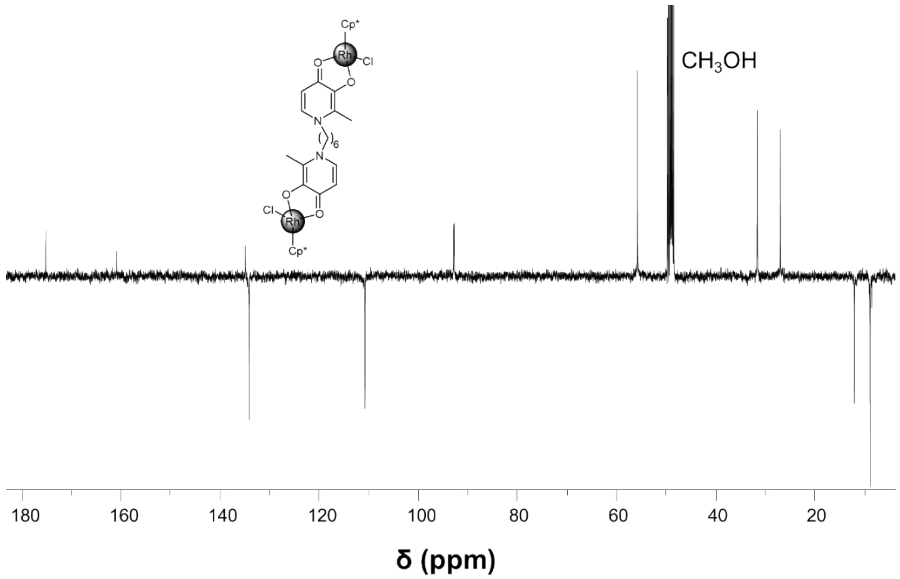

Figure S9. $^{13}C\{^{1}H\}$ NMR spectrum for **Rh^{6}** recorded in CD_3OD.

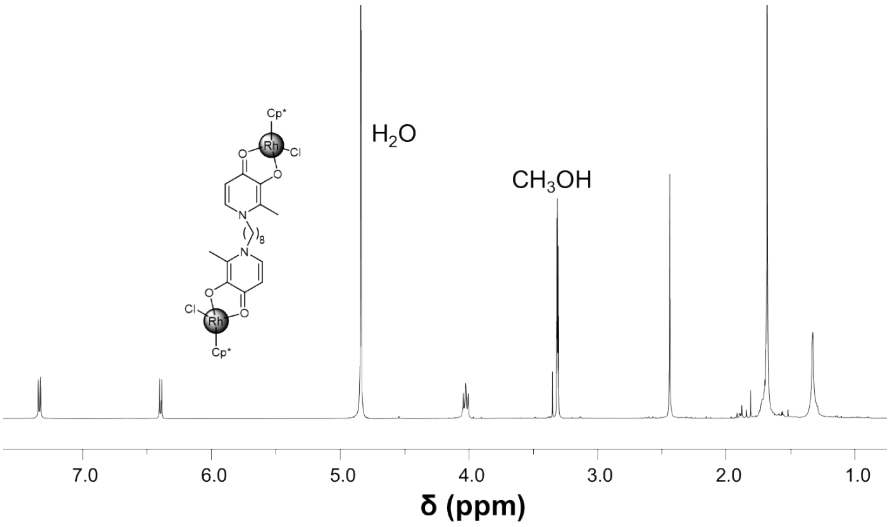

Figure S10. ^{1}H NMR spectrum for **Rh^{8}** recorded in CD_3OD.

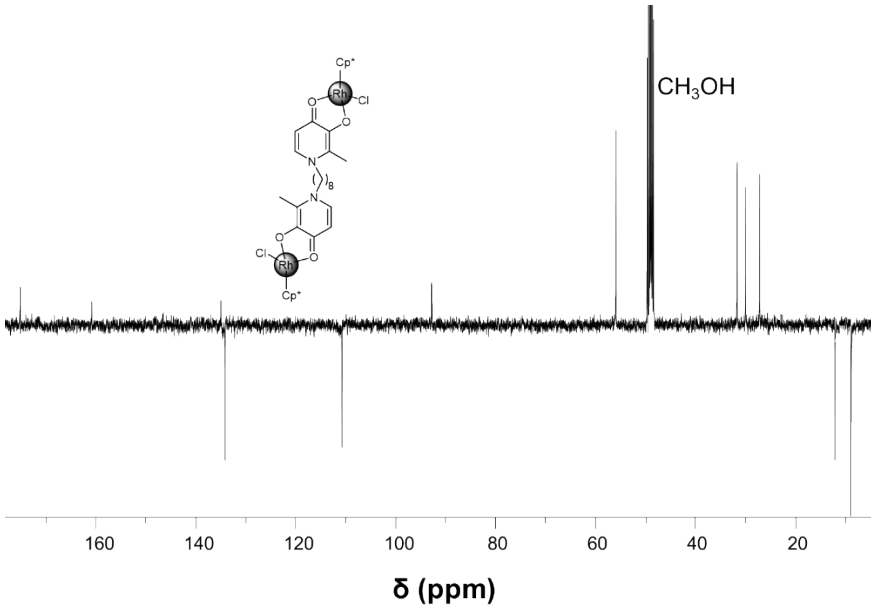

Figure S11. ^{13}C{^{1}H} NMR spectrum for **Rh^{8}** recorded in CD_3OD.

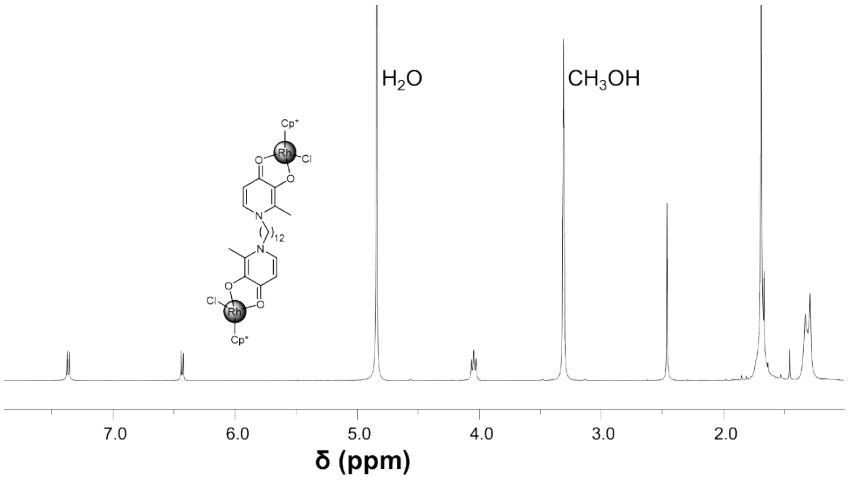

Figure S12. ^{1}H NMR spectrum for **Rh^{12}** recorded in CD_3OD.

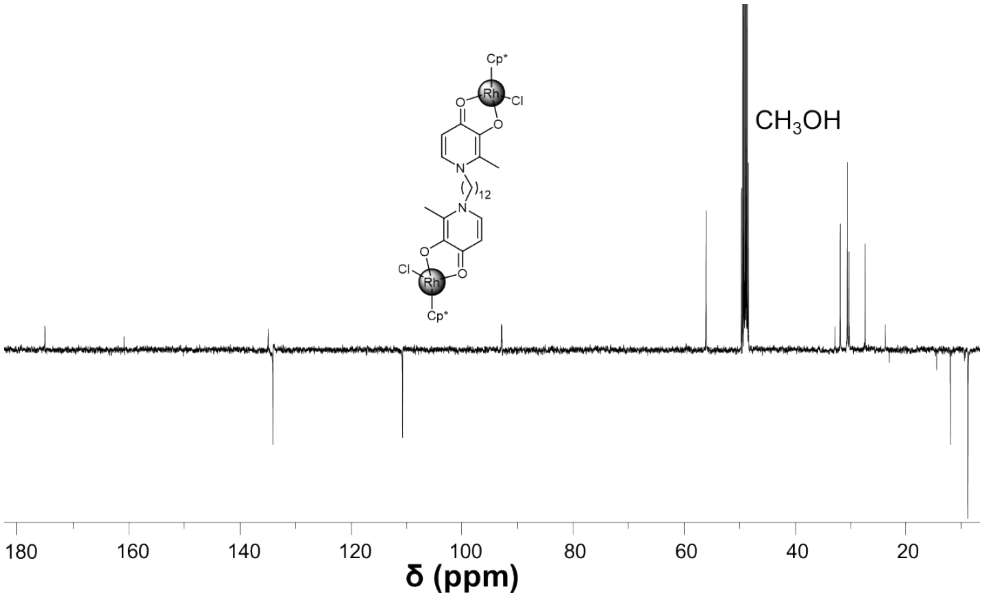

Figure S13. $^{13}C\{^{1}H\}$ NMR spectrum for **Rh^{12}** recorded in CD_3OD.

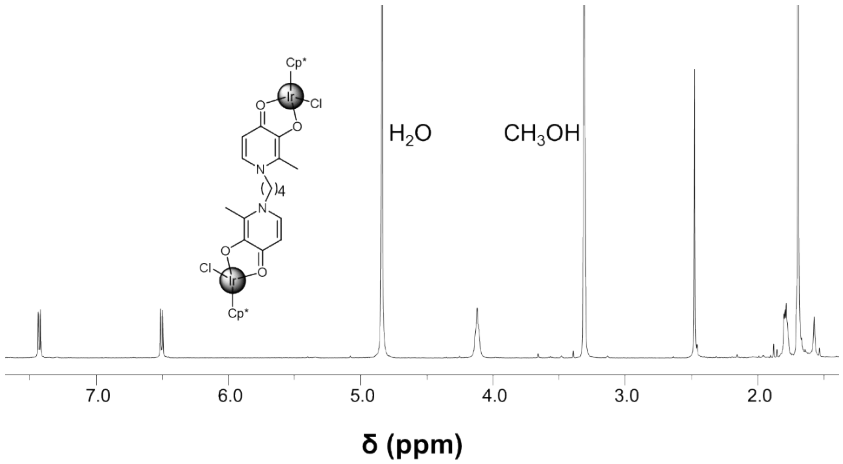

Figure S14. ^{1}H NMR spectrum for **Ir^{4}** recorded in CD_3OD.

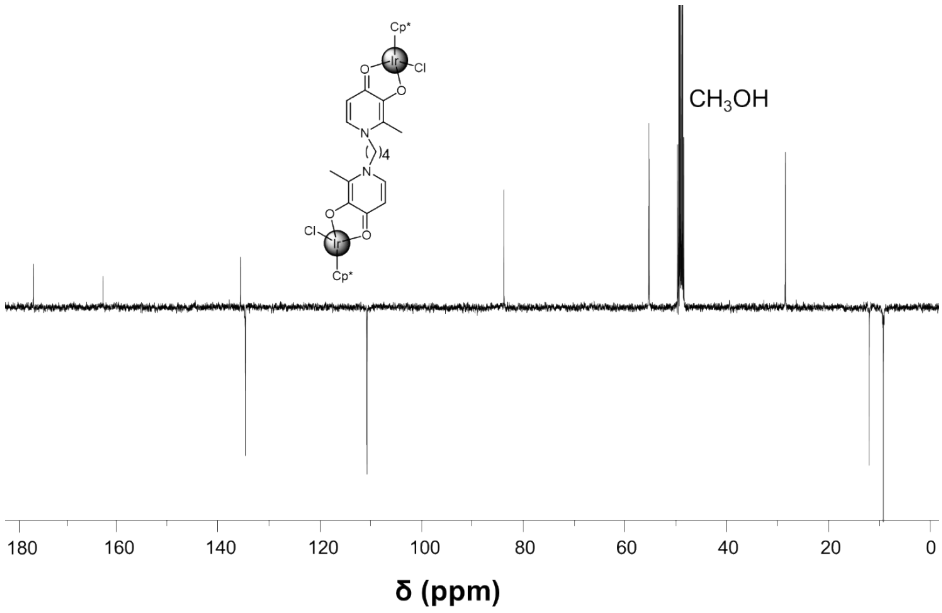

Figure S15. $^{13}C\{^{1}H\}$ NMR spectrum for **Ir^{4}** recorded in CD_3OD.

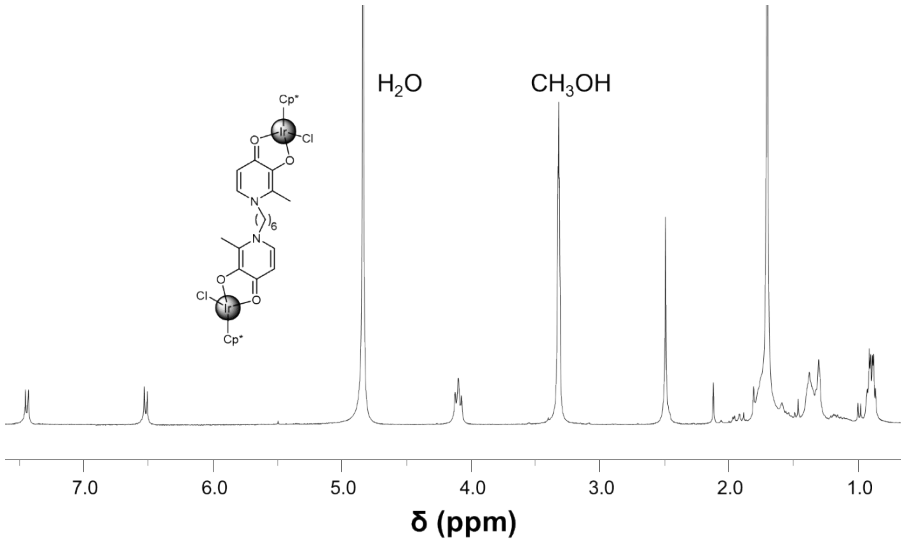

Figure S16. ^{1}H NMR spectrum for **Ir^{6}** recorded in CD_3OD.

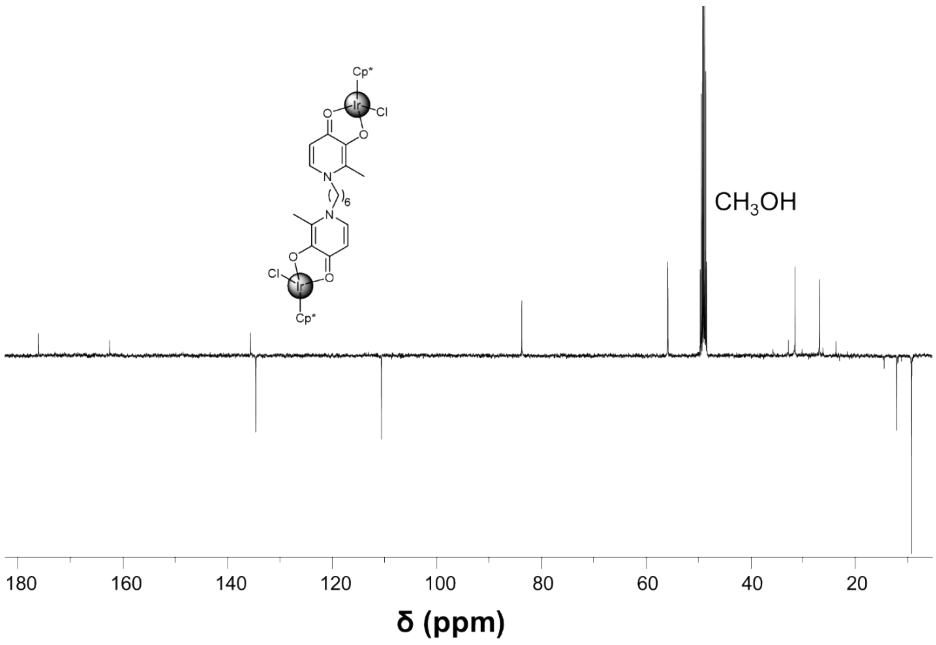

Figure S17. $^{13}C\{^{1}H\}$ NMR spectrum for **Ir^{6}** recorded in CD_3OD.

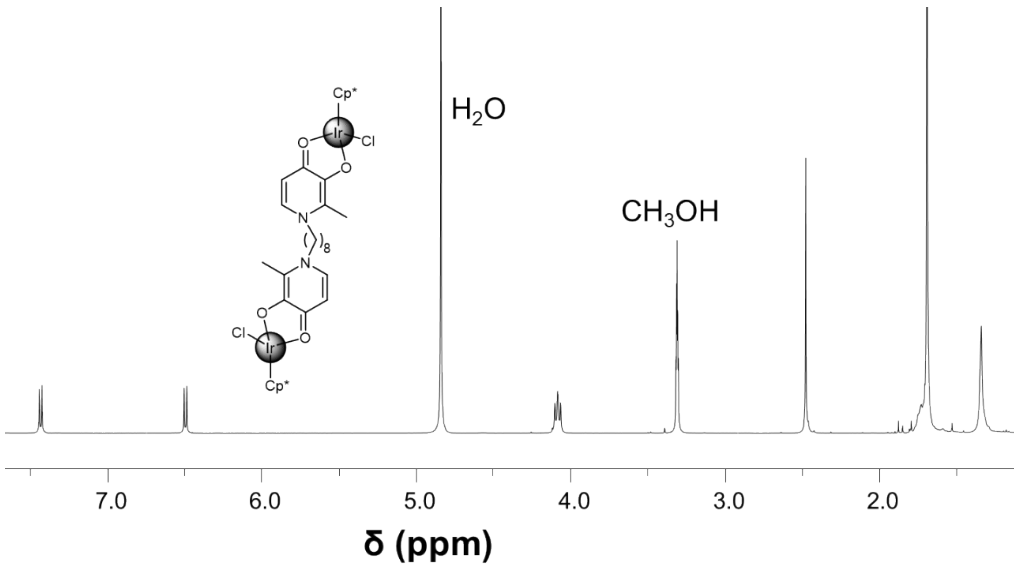

Figure S18. ^{1}H NMR spectrum for **Ir^{8}** recorded in CD_3OD.

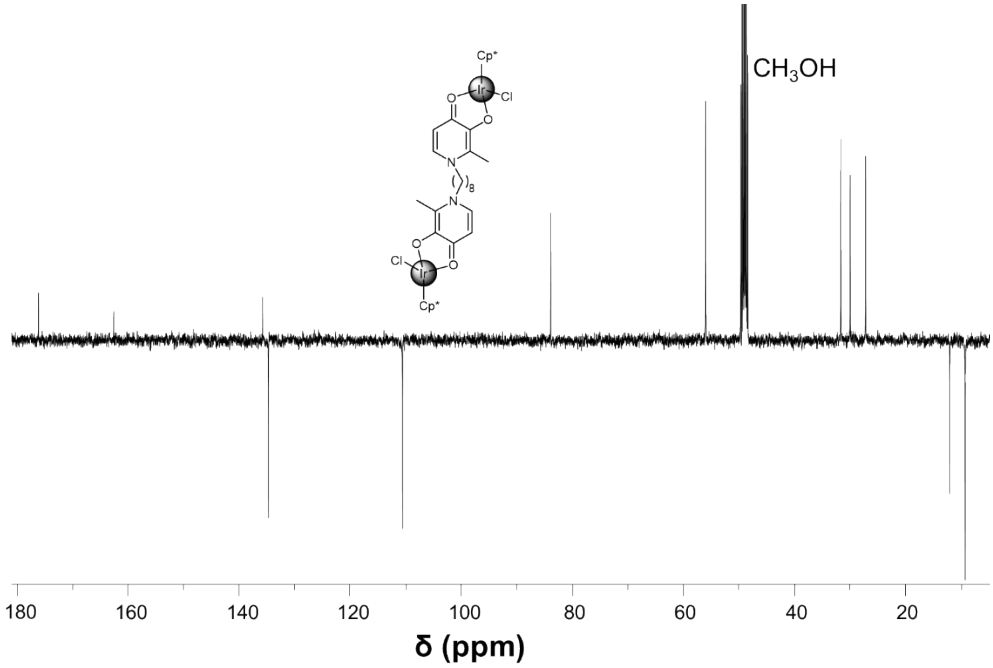

Figure S19. $^{13}C\{^{1}H\}$ NMR spectrum for **Ir^{8}** recorded in CD_3OD.

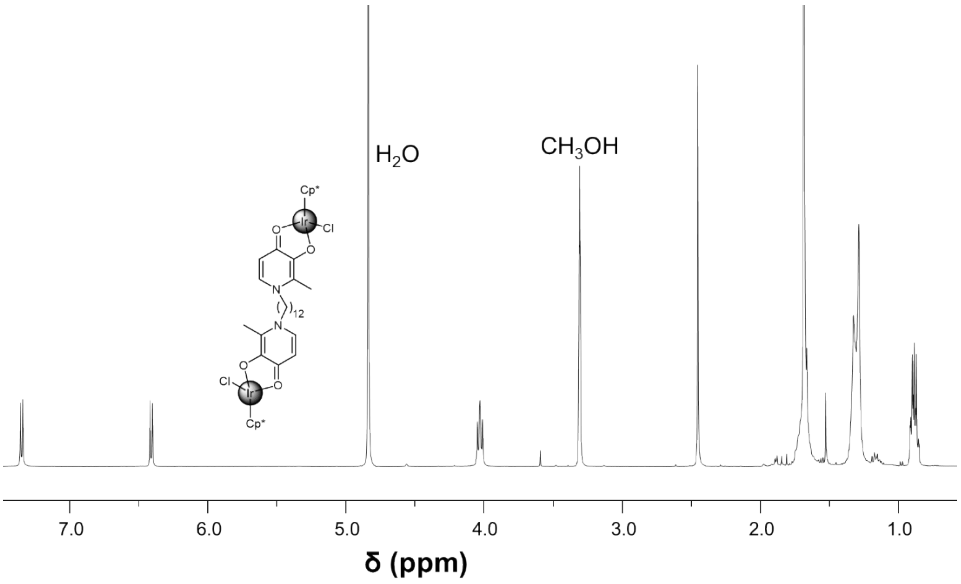

Figure S20. ^{1}H NMR spectrum for **Ir^{12}** recorded in CD_3OD.

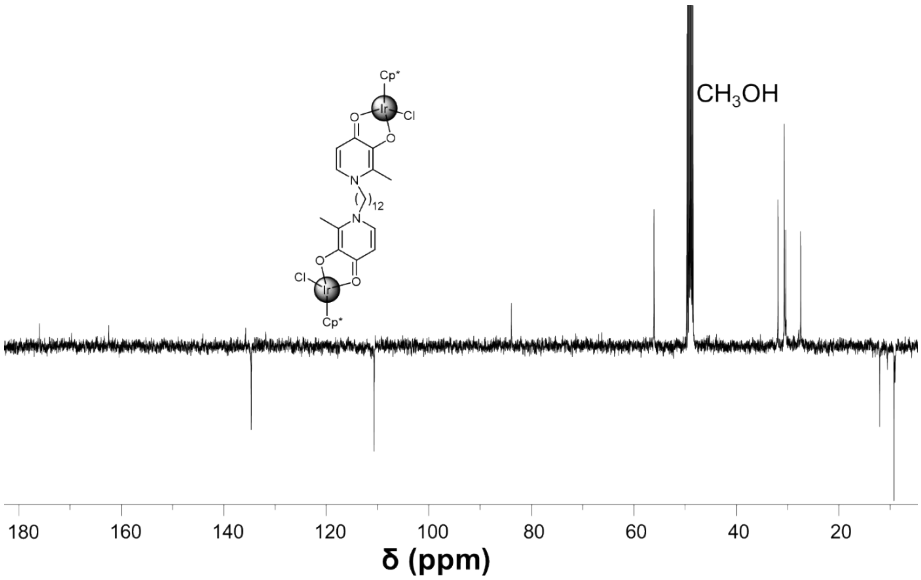

Figure S21. $^{13}C\{^{1}H\}$ NMR spectrum for **Ir^{12}** recorded in CD_3OD.

References

1 M. A. Bennett and A. K. Smith, *J. Chem. Soc., Dalton Trans.*, 1974, 233.

2 B. Booth, R. Haszeldine and M. Hill, *J. Chem. Soc. A*, 1969, 1299.

3 R. G. Ball, Graham, W. A. G., Heinekey, D. M., Hoyano, J. K., McMaster, A. D., Mattson, B. M., & Michel, S. T., *Inorg. Chem.*, 1990, **29**, 2023.

4 M. G. Mendoza-Ferri, C. G. Hartinger, M. A. Mendoza, M. Groessl, A. E. Egger, R. E. Eichinger, J. B. Mangrum, N. P. Farrell, M. Maruszak, P. J. Bednarski, F. Klein, M. A. Jakupec, A. A. Nazarov, K. Severin and B. K. Keppler, *J. Med. Chem.*, 2009, **52**, 916.

5 M. G. Mendoza-Ferri, C. G. Hartinger, A. A. Nazarov, W. Kandioller, K. Severin and B. K. Keppler, *Appl. Organomet. Chem.*, 2008, **22**, 326.

6 M. G. Mendoza-Ferri, C. G. Hartinger, R. E. Eichinger, N. Stolyarova, K. Severin, M. A. Jakupec, A. A. Nazarov and B. K. Keppler, *Organometallics*, 2008, **27**, 2405.

7 *SAINT, Area detector integration software*, Siemens Analytical Instruments Inc., Madison, WI, USA, 1995.

8 G. M. Sheldrick, *SADABS, Program for semi-empirical absorption correction*, University of Göttingen, Göttingen, Germany, 1997.

9 G. M. Sheldrick, *Acta Crystallogr., Sect. A: Found. Crystallogr.*, 2008, **A64**, 112.

10 O. V. Dolomanov, L. J. Bourhis, R. J. Gildea, J. A. Howard and H. Puschmann, *J. Appl. Crystallogr.*, 2009, **42**, 339.

11 A. Ashraf, F. Aman, S. Movassaghi, A. Zafar, M. Kubanik, W. A. Siddiqui, J. Reynisson, T. Sohnel, S. M. F. Jamieson, M. Hanif and C. G. Hartinger, *Organometallics*, 2019, **38**, 361.

12 E. Y. Leung, M. E. Askarian-Amiri, D. C. Singleton, C. Ferraro-Peyret, W. R. Joseph, G. J. Finlay, R. J. Brooms, P. M. Kakadia, S. K. Bohlander, E. Marshall and B. C. Baguley, *Front. Oncol.*, 2018, **8**.

13 J. Reynisson, J. K. Jaiswal, D. Barker, S. A. N. D'mello, W. A. Denny, B. C. Baguley and E. Y. Leung, *Cancer Cell Int.*, 2016, **16**, 18.

14 N. D. Lawson and B. M. Weinstein, *Dev. Biol.*, 2002, **248**, 307.

15 T. C. Y. Eng and J. W. Astin, *Methods Mol. Biol.*, 2018, **1846**, 71.